Published in final edited form as:
Cell Host Microbe. 2011 December 15; 10(6): 627–634. doi:10.1016/j.chom.2011.11.005.

Listeriolysin O suppresses Phospholipase C-mediated activation of the microbicidal NADPH oxidase to promote *Listeria monocytogenes* infection

Grace Y. Lam[1,3], **Ramzi Fattouh**[1], **Aleixo M. Muise**[1,2,3], **Sergio Grinstein**[1,3,4], **Darren E. Higgins**[6], and **John H. Brumell**[1,3,5,*]

[1]Cell Biology Program, Hepatology, and Nutrition, Hospital for Sick Children, Toronto, Ontario M5G 1X8, Canada

[2]Division of Gastroenterology, Hepatology, and Nutrition, Hospital for Sick Children, Toronto, Ontario M5G 1X8, Canada

[3]Institute of Medical Science, University of Toronto, Toronto, ON M5S1A8, Canada

[4]Department of Biochemistry, University of Toronto, Toronto, ON M5S1A8, Canada

[5]Department of Molecular Genetics, University of Toronto, Toronto, ON M5S1A8, Canada

[6]Department of Microbiology and Immunobiology, Harvard Medical School, Boston, MA 02115, USA

Summary

The intracellular bacterial pathogen *Listeria monocytogenes* produces phospholipases C (PI-PLC and PC-PLC) and the pore-forming cytolysin listeriolysin O (LLO) to escape the phagosome and replicate within the host cytosol. We found that PLCs can also activate the phagocyte NADPH oxidase during *L. monocytogenes* infection, a response that would adversely affect pathogen survival. However, secretion of LLO inhibits the NADPH oxidase by preventing its localization to phagosomes. LLO-deficient bacteria can be complemented by perfringolysin O, a related cytolysin, suggesting that other pathogens may also use pore-forming cytolysins to inhibit the NADPH oxidase. Our studies demonstrate that while the PLCs induce antimicrobial NADPH oxidase activity, this effect is alleviated by the pore-forming activity of LLO. Therefore, the combined activities of PLCs and LLO on membrane lysis and the inhibitory effects of LLO on NADPH oxidase activity allows *L. monocytogenes* to efficiently escape the phagosome while avoiding the microbicidal respiratory burst.

Introduction

Listeria monocytogenes is a Gram-positive bacterial pathogen that has adapted to intracellular infection within its host (Schnupf and Portnoy, 2007). Upon entry into host cells, bacteria can escape from the phagosome through the activity of three virulence factors, listeriolysin O (LLO), a phosphatidylinositol-specific phospholipase C (PI-PLC) and a

*Corresponding author: Dr. John H. Brumell, Cell Biology Program, Hospital for Sick Children, 555 University Avenue, Toronto, ON, Canada, M5G 1X8, Tel: (416) 813-7654 ext. 3555, FAX: (416) 813-5028, john.brumell@sickkids.ca.

broad-range phospholipase C (PC-PLC). The pore-forming activity of LLO has been shown to prevent acidification of phagosomes in macrophages, thereby delaying their fusion with lysosomes prior to mediating phagosome escape (Shaughnessy et al., 2006). PLCs have been shown to directly disrupt membranes through hydrolysis of phospholipids, and in part through the activation of signal transduction cascades as a result of diacylglycerol production (Goebel and Kuhn, 2000; Goldfine et al., 1993). Thus, these virulence factors contribute to the ability of *L. monocytogenes* to escape from the phagosome by different mechanisms.

The NOX2 nicotinamide adenine dinucleotide phosphate (NADPH) oxidase (also referred to as gp91^{phox}; phagocyte oxidase) plays a key role in immune responses via the production of reactive oxygen species (ROS) (Lam et al., 2010). The loss of NADPH oxidase activity in mice lacking the gp91^{phox} subunit (gp91$^{phox-/-}$) results in increased replication of *L. monocytogenes* during the first 24 h of infection compared to wild type animals (Dinauer et al., 1997; Shiloh et al., 1999). *In vitro* studies suggest that the NOX2 NADPH oxidase limits escape of *L. monocytogenes* from the phagosome in macrophages (Myers et al., 2003).

To ensure survival in host cells, a number of pathogens have evolved mechanisms to inhibit ROS production by the NOX2 NADPH oxidase (Allen et al., 2005; Blanchard et al., 2003; Boncompain et al., 2010; Keith et al., 2009; McCaffrey and Allen, 2006; Mott et al., 2002; Siemsen et al., 2009). *Salmonella enterica* serovar Typhimurium has been shown to inhibit NOX2 NADPH oxidase delivery to bacteria-containing phagosomes (Vazquez-Torres et al., 2000). However, total cellular ROS production by the NOX2 NADPH oxidase is unaffected in *Salmonella*-infected cells. These findings indicate that local inhibition of the NOX2 NADPH oxidase at phagosomes allows intracellular growth of these bacteria. The virulence factors used by *Salmonella* to mediate this phenotype are not known. Indeed, despite intensive research in this area, the mechanisms by which bacterial pathogens alter NOX2 NADPH oxidase activity during infection remain unclear.

Previously, it was shown that *L. monocytogenes*-infected neutrophils generate ROS 10 min post-infection (p.i.) (Sibelius et al., 1999). However, exploration of the dynamics and localization of ROS production during *L. monocytogenes* infection have been limited. Since *L. monocytogenes* escape from the phagosome is a slow process (beginning 30 min p.i.) (de Chastellier and Berche, 1994), Alvarez-Dominguez and colleagues suggested that these bacteria may employ mechanisms to inhibit the NADPH oxidase during infection (Prada-Delgado et al., 2001). However, this hypothesis remains untested. Owing to the importance of the NOX2 NADPH oxidase in innate immunity, we examined ROS production in *L. monocytogenes*-infected macrophages, a cell type colonized by these bacteria during systemic infection. We demonstrate that *L. monocytogenes*, via the activity of LLO, can inhibit phagosomal production of ROS by the NOX2 NADPH oxidase.

Results

LLO inhibits intracellular ROS production by the NOX2 NADPH oxidase

We performed dynamic measurements of intracellular and extracellular ROS production in bone marrow-derived macrophages (BMDM) using luminol or isoluminol, respectively (Figure 1A and 1B). During infection by wild type *L. monocytogenes*, both intracellular and extracellular ROS production peaked at 10 min p.i. and decreased at later time points (Figure 1A and 1B). Treatment of cells with phorbol 12-myristate 13-acetate (PMA), a known activator of the NOX2 NADPH oxidase, served as a positive control (Table S1A and S1B). These findings demonstrate that *L. monocytogenes* can induce rapid activation of the NOX2 NADPH oxidase in leukocytes, consistent with previous observations (Sibelius et al., 1999).

Given that oxidative stress results in an upregulation of LLO (Makino et al., 2005), a virulence factor that inhibits phagosome maturation (Shaughnessy et al., 2006), we hypothesized that LLO may participate in a specific bacterial response to ROS. To test this hypothesis, we examined ROS production in cells infected with LLO-deficient bacteria (ΔLLO, lacking the *hly* gene). We observed significantly higher intracellular ROS production in ΔLLO infected cells compared to wild type infected cells at 40-70 min p.i. (Figure 1A and Table S1A). Addition of the flavoprotein inhibitor diphenyliodonium (DPI, a known NADPH oxidase inhibitor) prevented ROS production in ΔLLO infected cells (Table S1A and S1B). In contrast, the kinetics of extracellular ROS production were similar upon infection with wild type or ΔLLO *L. monocytogenes* (Figure 1B, Table S1B). These observations suggest that LLO inhibits intracellular ROS production.

We further examined intracellular ROS production using 5-(and-6)-chloromethyl-2-7-dichlorodihydrofluorescein diacetate (CM-H_2DCFDA) in RAW 264.7 macrophages. Cells were stimulated with PMA, or infected with either wild type or ΔLLO bacteria, CM-H_2DCFDA was added 30 min p.i. and the cells examined by flow cytometry at 1 h p.i. As expected, treatment of cells with PMA resulted in robust ROS production (Figure 1C and 1D). Consistent with the luminol assay, we observed little ROS production in wild type infected cells but high levels of ROS production in ΔLLO infected cells, comparable to those attained by stimulation with PMA (Figure 1C and 1D). We also measured intracellular superoxide production using the nitroblue tetrazolium (NBT) reduction assay. ΔLLO bacteria induced a marked production of superoxide in RAW 264.7 macrophages, while infection with wild type bacteria did not (Figure S1A).

To further examine the role of LLO, we employed an LLO-deficient strain that inducibly expresses LLO (iLLO) in response to isopropyl β-D-1-thiogalactopyranoside (IPTG). In the absence of IPTG, iLLO bacteria triggered ROS production. However, in the presence of IPTG, iLLO bacteria produced significantly less ROS upon infection (Figure S1A). Addition of purified LLO to human neutrophils was sufficient to inhibit PMA-induced ROS production (Figure S1B) at concentrations that did not cause cell toxicity (Figure S1C). Therefore, LLO is both necessary and sufficient for inhibition of intracellular ROS production by the NADPH oxidase.

To visualize the localization of ROS production during *L. monocytogenes* infection, we employed transmission electron microscopy (TEM) with cerium chloride. IgG-coated 3.8 μm latex beads were fed to RAW 264.7 macrophages as positive controls of phagosomal ROS production. A dark cerium precipitate was observed in phagosomes containing latex beads, indicative of ROS production in this compartment (Figure 2A, 2B and 2G); accordingly, formation of the precipitate was inhibited by DPI treatment (Figure 2C, 2D and 2G). ROS production was not observed in phagosomes containing wild type *L. monocytogenes* (Figure 2F and 2G). However, marked cerium precipitation was observed in phagosomes containing ΔLLO bacteria (Figure 2E and 2G). Together, these results indicate that LLO inhibits NOX2 NADPH oxidase-dependent ROS production in the phagosome.

L. monocytogenes PLCs contribute to the induction of ROS production by the NOX2 NADPH oxidase

The observation that ΔLLO bacteria induced high levels of intracellular ROS production, comparable to those observed in cells treated with PMA, suggested that bacterial products have the capacity to promote NOX2 NADPH oxidase activity in the absence of LLO. It was previously shown that PLCs from *Clostridium perfringens, Pseudomonas aeruginosa* and *Bacillus cereus* are linked to activation of the NOX2 NADPH oxidase (Styrt et al., 1989; Titball, 1993). These enzymes generate diacylglycerol, a cofactor for activation of protein kinase C (PKC), which contributes to NOX2 NADPH oxidase activation via the

phosphorylation of p47^{phox} (Fontayne et al., 2002). Similarly, *L. monocytogenes* PLCs have been shown to generate diacylglycerol and activate PKC during infection of macrophages (Camilli et al., 1993; Goldfine et al., 1993). Therefore we hypothesized that *L. monocytogenes* PLCs may activate the NOX2 NADPH oxidase in the absence of LLO.

To test this hypothesis, we examined whether *L. monocytogenes* PLCs are required for ROS production. In contrast to ΔLLO bacteria, a strain lacking LLO and both PLCs (ΔLLO ΔPI-PLC ΔPC-PLC; lacking *hly, plcA* and *plcB* genes) produced little intracellular ROS (Table S1A and Figure 1D). Similarly, ROS production was not observed in phagosomes containing ΔLLO ΔPI-PLC ΔPC-PLC bacteria as determined by the cerium precipitation assay (Figure 2G). Infection with a strain that lacks both PLCs (ΔPI-PLC ΔPC-PLC), but expressing LLO, resulted in ROS production comparable to that of wild type bacteria (Figure 1D). These results indicate that LLO inhibits PLC-mediated NOX2 NADPH oxidase-dependent ROS production in the phagosome.

Next, we treated cells with purified PI-PLC and observed a significant induction of ROS production that was inhibited by the PKC inhibitors Rottlerin and GÖ6983 (Figure 1E). ROS production by PI-PLC was also inhibited by concurrent treatment with purified LLO. These results suggest that PI-PLC is sufficient to drive NOX2 NADPH oxidase activation by stimulating PKC and that LLO is sufficient to inhibit this deleterious consequence of PLC activity. This is consistent with a previous finding that *L. innocua* expressing PI-PLC induces greater ROS production than wild type *L. innocua* in neutrophils (Sibelius et al., 1999). However, *L. monocytogenes* mutants that only express PI-PLC (and not PC-PLC or LLO) or PC-PLC (and not PI-PLC or LLO) do not induce significant ROS production (Figure S1D). These observations suggest that both PLCs are required to mediate ROS production in the context of *L. monocytogenes* infection. However, higher doses of PI-PLC may be sufficient to drive NOX2 NADPH oxidase activation. Collectively, our results suggest that bacterial PLCs induce intracellular ROS production and that LLO inhibits this deleterious consequence of PLC activity.

LLO-deficient bacteria survive in NOX2 NADPH oxidase-deficient macrophages

The relevance of LLO-mediated inhibition of the NOX2 NADPH oxidase to intracellular *L. monocytogenes* survival/replication was determined by gentamicin protection assays using BMDM isolated from C57BL/6 and gp91$^{phox-/-}$ mice. The number of intracellular ΔLLO bacteria decreased over time in C57BL/6 BMDM (Figure 3A), consistent with previous observations (Alberti-Segui et al., 2007). In contrast, ΔLLO bacteria displayed extended survival in gp91$^{phox-/-}$ BMDM (Figure 3A). Wild type *L. monocytogenes* replicated at a similar rate in both C57BL/6 and gp91$^{phox-/-}$ BMDM (Figure 3B). ΔLLO bacteria that were complemented by expression of LLO (ΔLLO + LLO) displayed a similar replication profile as that of wild type bacteria (Figure S2A).

LLO-deficient bacteria survive in NOX2 NADPH oxidase-deficient mice

The *in vivo* relevance of LLO-mediated inhibition of the NOX2 NADPH oxidase was examined in C57BL/6 and gp91$^{phox-/-}$ mice. Wild type *L. monocytogenes* replicated significantly over the course of 24 h in both C57BL/6 and gp91$^{phox-/-}$ mice (Figure S2B). The bacterial load at 24 h was higher in gp91$^{phox-/-}$ compared to C57BL/6 mice (Figure S2B and S2C), as previously reported (Dinauer et al., 1997). However, clearance of ΔLLO bacteria was significantly impaired in the gp91$^{phox-/-}$ mice as compared to C57BL/6 mice (Figure 3C and 3D). Consistent with this result, more granulomas were observed at 24 h post-infection in the livers of gp91$^{phox-/-}$ mice infected with ΔLLO bacteria than in C57BL/6 mice (Figure 3E). These results indicate that LLO-mediated inhibition of NADPH oxidase activity is required for *L. monocytogenes* survival both *in vitro* and *in vivo*.

LLO inhibits NOX2 NADPH oxidase assembly at the phagosome

The NOX2 NADPH oxidase is composed of a transmembrane heterodimer of gp91^{phox} and p22^{phox}, and regulatory cytosolic subunits, including p40^{phox}, p47^{phox}, p67^{phox} and the small GTPase Rac2. We hypothesized that LLO inhibits ROS production by preventing proper localization of NOX2 NADPH oxidase components to the phagosome. To test this hypothesis, human primary macrophages were infected with GFP-expressing wild type or ΔLLO bacteria and immunostained for p22^{phox} (Figure 4B), p47^{phox} or p67^{phox} (Figure S3). IgG-opsonized sheep red blood cells were employed as a positive control for localization of the NOX2 NADPH oxidase to phagosomes (Figure 4A, S3A and S3C). We observed minimal colocalization between intracellular wild type bacteria and the NOX2 NADPH oxidase components tested (Figure 4B, 4C, S3B and S3D). In contrast, we observed more than a three-fold increase in co-localization between intracellular ΔLLO bacteria and all of the NOX2 NADPH oxidase components tested (Figure 4B, 4C, S3B and S3D). These observations demonstrate that LLO prevents NOX2 NADPH oxidase assembly at the phagosome.

Perfringolysin O (PFO) expression can complement NOX2 NADPH oxidase inhibition by LLO deficient bacteria

We next determined whether, like LLO, other bacterial pore-forming cytolysins could also inhibit the NOX2 NADPH oxidase. We used ΔLLO bacteria expressing perfringolysin O (PFO) from *C. perfringens* under a tightly controlled IPTG-inducible promoter (iPFO). In the absence of IPTG, iPFO-infected cells generated significant amounts of superoxide, similar to ΔLLO (Figure 4D). However, upon IPTG induction, superoxide production was inhibited. The same effect was observed in bacteria-containing phagosomes by TEM analysis of cerium precipitates (Figure 4E). Since PFO can complement LLO for inhibition of NOX2 NADPH oxidase, these results suggest that the inhibition of ROS production may be a common strategy used by other bacteria that secrete pore-forming cytolysins.

Discussion

Here we provide evidence that *L. monocytogenes* can modulate intracellular NOX2 NADPH oxidase activity during infection. Upon invasion, *L. monocytogenes* produces PLCs and LLO, which mediate bacterial phagosome escape. Production of diacylglycerol by PLCs has been implicated in phagosome escape by *L. monocytogenes* (Grundling et al., 2003). However, diacylglycerol can also activate the NOX2 NADPH oxidase through activation of PKC (Dang et al., 2001). Therefore, the induction of antibacterial ROS by PLCs is a potentially deleterious consequence of the mechanism that the bacteria utilize to promote phagosome escape in host cells. Here we show that ROS production between 40-70 min p.i. can be triggered by bacterial PLCs during infection by ΔLLO bacteria. The mechanism(s) by which bacterial PLCs contribute to NADPH oxidase activation in phagosomes remain to be established.

Countering the potentially deleterious effect of PLCs, we find that LLO plays a key role in inhibiting the NOX2 NADPH oxidase between 40-70 min p.i. by blocking its localization to phagosomes. Therefore, one consequence of LLO pore formation is inhibition of PLC-stimulated ROS production, in addition to its role in phagosome escape and other virulence functions (Schnupf and Portnoy, 2007). We find that LLO has no significant impact on ROS production at 10 min p.i. (Figure 1A, 1B, Table S1A, S1B), which is known to be mediated, at least in part, through *L. monocytogenes* peptidoglycan stimulation (Remer et al., 2005). In contrast to our findings, expression of LLO by *L. innocua* was found to enhance ROS production during 10 min infection of human neutrophils (Sibelius et al., 1999), so we

cannot rule out the possibility that LLO may activate the NADPH oxidase under some experimental conditions.

How does LLO inhibit the NADPH oxidase in phagosomes? To begin to explore this question, we examined signaling events linked to activation of the NADPH oxidase in *L. monocytogenes* infected cells. We observed phosphorylation of the $p40^{phox}$ subunit of the NADPH oxidase occurs in macrophages infected with both wild type and ΔLLO bacteria (Figure S4A). The activities of p38, AKT, ERK1/2 and PKCδ are required for NADPH oxidase activity (Bey et al., 2004; Chen et al., 2003; Dang et al., 2003; Dekker et al., 2000; Dewas et al., 2000; Fontayne et al., 2002). However, we observed variability in these responses and our results from three independent experiments did not show any significant differences in the activation of these kinases (as judged by phosphorylation of active-site residues) between wild type or ΔLLO infected macrophages (Figure S4B-E). These findings indicate that LLO does not block the signaling that leads to NADPH oxidase activation, and instead suggest that it inhibits localization of the oxidase to phagosomes. Indeed, this is consistent with our observation that extracellular ROS production by the NADPH oxidase activation is not affected by LLO during *L. monocytogenes* infection (Figure 1B, Table S1B).

It is intriguing that both *L. monocytogenes* (reported here) and *Salmonella enterica* serovar Typhimurium (Vazquez-Torres et al., 2000) have evolved mechanisms to inhibit NADPH oxidase activity at phagosomes, allowing their intracellular colonization, but without globally disrupting ROS production by this system. It is possible that both pathogens exploit extracellular ROS-mediated signaling to promote inflammatory responses while inhibiting locally the microbicidal actions of these molecules.

These studies reveal how *L. monocytogenes* initiates a dynamic, and in this case antagonistic, set of signals in host cells via its virulence factors to allow for optimal bacterial growth and survival during infection. The observation that PFO can also mediate a similar inhibition of NOX2 NADPH oxidase suggests that inhibition of ROS production may be a conserved consequence of pore-forming cytolysin activity. Since PLCs and pore-forming cytolysins are encoded by a wide range of bacterial pathogens, this model may be applicable to several pathogenic species.

Experimental Procedures

Bacterial strains and culture conditions

The *L. monocytogenes* strains used are listed in Supplemental Data.

Macrophage generation and culture conditions

RAW 264.7 macrophages were purchased from American Type Culture Collection (Rockville, MD). RAW 264.7 cells were maintained in DMEM growth medium (HyClone) supplemented with 10% FBS (Wisent) at 37°C in 5% CO_2 without antibiotics.

All experimental protocols involving mice were approved by the Animal Care Committee of The Hospital for Sick Children. Mice were euthanized by cervical dislocation. For BMDM, the femur and tibia were removed, cleansed of muscle fibers and cut distally. The bone marrow was then removed via a 10 sec pulse of centrifugation at 2000 rpm. The resulting cells were centrifuged at 1500 rpm for 5 min, washed with growth media and plated on 10 cm tissue culture dishes. Media was replaced with fresh RPMI growth media (see below) every 3 days. Typically, 10^8 bone marrow-derived macrophages (BMDM) were typically recovered after 7 days. Murine macrophages were maintained in RPMI-1640 medium (Wisent) supplemented with 10% FBS (Wisent), 5% sodium pyruvate (Invitrogen), 5% pen/

strep (Invitrogen), 5% non-essential amino acids (Invitrogen) and 0.5 μM β-mercaptoethanol (Invitrogen). BMDMs were differentiated in 30% L929 conditioned media. L929 conditioned medium was generated by growing L929 cells (ATCC) in 150-cm^2 flasks at an initial density of 1×10^8 cells per flask in growth media as described above for use with RAW 264.7 cells. After 3 days, confluency was reached and the growth media was substituted with DMEM alone. After 7-10 days, culture supernatant was collected and centrifuged at 1,500 rpm for 5 mins, aliquoted and stored at -20°C. Human macrophages were prepared as previously described (McGilvray et al., 2000).

In vivo infection

Three to five week old C57BL/6J and gp91$^{phox-/-}$ (*Cybb/tm1d*) mice were purchased from Jackson Laboratory. Mice were infected via intravenous injection in the lateral tail vein with wild type *L. monocytogenes* at 5×10^4 CFU in 200 μl of PBS, and ΔLLO bacteria at 1×10^9 CFU in 200 μl of PBS. Mice were sacrificed at indicated time points and the livers were obtained. The right lobes of the livers were fixed with formalin, embedded and 3μm sections were stained with hematoxylin and eosin (H&E). The left lobes were homogenized in sterile PBS for CFU quantification from serial dilutions on BHI-agar plates.

Macrophage replication assay and infection

After 7-10 days of differentiation, BMDM were washed twice and detached with ice cold Versene Buffer (0.8 mM EDTA, 1 mM glucose in PBS$^{-/-}$) for 20 min at 4°C and plated at 5×10^5 cells per well in 24-well tissue culture plates, 24 h prior to infection. All strains of *L. monocytogenes* were infected at a multiplicity of infection (MOI) of 1. After 30 min of invasion at 37°C, cells were washed three times with phosphate buffered saline (PBS) followed by the addition of DMEM. At 1 h post-infection, media was changed and growth media containing 50 μg/ml gentamicin was added. Cells were then lysed at 2, 4, 8, 12, and 24 h post-infection with 0.2% TritonX-100 in PBS$^{+/+}$. Serial dilutions of the lysates were plated on BHI-agar plates and incubated 14-16 h for subsequent quantification of colony forming units (CFUs).

Immunofluorescence and antibodies

Immunostaining was conducted as previously described (Brumell et al., 2001). In brief, after infections, human macrophages were fixed using 2.5% paraformaldehyde for 10 min at 37°C. Extracellular *L. monocytogenes* were detected by immunostaining prior to permeabilization. Cells were then permeabilized and blocked using 0.2% saponin with 10% normal goat serum 14-16 h at 4°C and staining for intracellular bacteria, p22^{phox}, p47^{phox} and p67^{phox} was completed using mouse anti-GFP, rabbit anti-p22^{phox} (gift from Dr. Mark T. Quinn, Montana State University), rabbit anti-p47^{phox} and rabbit anti-p67^{phox} (gifts from Nathalie Grandvaux, McGill University). All fluorescent secondary antibodies were AlexaFluor conjugates from Molecular Probes (Invitrogen). All colocalization quantifications and image acquisitions of sRBC fed cells were done using a Leica DMIRE2 epifluorescence microscope equipped with a 100× oil objective, 1.4 numerical aperture. Images of WT and ΔLLO infected cells are confocal *z* slices taken using a Zeiss Axiovert confocal microscope and LSM 510 software. Volocity software (Improvision) was used to analyse images. Images were imported into Adobe Photoshop and assembled in Adobe Illustrator.

Statistical Analysis

Statistical analyses were conducted using GraphPad Prism v4.0a. The mean ± standard error (SEM) is shown in figures, and *P* values were calculated using two-tailed two-sample equal variance Student's *t*-test unless otherwise stated. A p-value of less than 0.05 was considered

statistically significant and is denoted by *. $p < 0.01$ is denoted by ** and $p < 0.005$ is denoted by ***.

Supplementary Material

Refer to Web version on PubMed Central for supplementary material.

Acknowledgments

We are grateful to Dr. Dan Portnoy for generously providing bacterial strains. We thank Drs. L. A. Allen, M. Dinauer, H. Goldfine, N. Grandvaux, H. Marquis, and M. Quinn for kindly providing reagents and technical advice. We also thank Michelle Ang and David Rittuzi for their assistance with FACS, Robert Tempkin for his assistance with TEM and Mike Woodside and Paul Paroutis for their support with microscopy. Finally, the authors would like to thank Dr. Mathew Estey for critical reading of the manuscript. John H. Brumell, PhD holds an Investigators in Pathogenesis of Infectious Disease Award from the Burroughs Wellcome Fund. Infrastructure for the Brumell Laboratory was provided by a New Opportunities Fund from the Canadian Foundation for Innovation and the Ontario Innovation Trust. G.Y.L. is supported by a M.D/Ph.D Studentship and Canadian Graduate Scholarship Doctoral Research Award from the Canadian Institutes of Health Research. R.F is supported by a ResTraComp fellowship from the Hospital for Sick Children. This work was supported by operating grants from the Canadian Institutes of Health Research (MOP#97756), The Arthritis Society of Canada (#RG11/013) and a United States Public Health Service grant (AI053669) from the National Institutes of Health (D.E.H.).

References

Alberti-Segui C, Goeden KR, Higgins DE. Differential function of Listeria monocytogenes listeriolysin O and phospholipases C in vacuolar dissolution following cell-to-cell spread. Cell Microbiol. 2007; 9:179–195. [PubMed: 17222191]

Allen LA, Beecher BR, Lynch JT, Rohner OV, Wittine LM. Helicobacter pylori disrupts NADPH oxidase targeting in human neutrophils to induce extracellular superoxide release. Journal of immunology. 2005; 174:3658–3667.

Bey EA, Xu B, Bhattacharjee A, Oldfield CM, Zhao X, Li Q, Subbulakshmi V, Feldman GM, Wientjes FB, Cathcart MK. Protein kinase C delta is required for p47phox phosphorylation and translocation in activated human monocytes. J Immunol. 2004; 173:5730–5738. [PubMed: 15494525]

Blanchard TG, Yu F, Hsieh CL, Redline RW. Severe inflammation and reduced bacteria load in murine helicobacter infection caused by lack of phagocyte oxidase activity. J Infect Dis. 2003; 187:1609–1615. [PubMed: 12721941]

Boncompain G, Schneider B, Delevoye C, Kellermann O, Dautry-Varsat A, Subtil A. Production of reactive oxygen species is turned on and rapidly shut down in epithelial cells infected with Chlamydia trachomatis. Infect Immun. 2010; 78:80–87. [PubMed: 19858301]

Brumell JH, Rosenberger CM, Gotto GT, Marcus SL, Finlay BB. SifA permits survival and replication of Salmonella typhimurium in murine macrophages. Cell Microbiol. 2001; 3:75–84. [PubMed: 11207622]

Camilli A, Tilney LG, Portnoy DA. Dual roles of plcA in Listeria monocytogenes pathogenesis. Mol Microbiol. 1993; 8:143–157. [PubMed: 8388529]

Chen Q, Powell DW, Rane MJ, Singh S, Butt W, Klein JB, McLeish KR. Akt phosphorylates p47phox and mediates respiratory burst activity in human neutrophils. J Immunol. 2003; 170:5302–5308. [PubMed: 12734380]

Dang PM, Fontayne A, Hakim J, El Benna J, Perianin A. Protein kinase C zeta phosphorylates a subset of selective sites of the NADPH oxidase component p47phox and participates in formyl peptide-mediated neutrophil respiratory burst. J Immunol. 2001; 166:1206–1213. [PubMed: 11145703]

Dang PM, Morel F, Gougerot-Pocidalo MA, El Benna J. Phosphorylation of the NADPH oxidase component p67(PHOX) by ERK2 and P38MAPK: selectivity of phosphorylated sites and existence of an intramolecular regulatory domain in the tetratricopeptide-rich region. Biochemistry. 2003; 42:4520–4526. [PubMed: 12693948]

de Chastellier C, Berche P. Fate of Listeria monocytogenes in murine macrophages: evidence for simultaneous killing and survival of intracellular bacteria. Infect Immun. 1994; 62:543–553. [PubMed: 8300212]

Dekker LV, Leitges M, Altschuler G, Mistry N, McDermott A, Roes J, Segal AW. Protein kinase C-beta contributes to NADPH oxidase activation in neutrophils. Biochem J. 2000; 347(Pt 1):285–289. [PubMed: 10727429]

Dewas C, Fay M, Gougerot-Pocidalo MA, El-Benna J. The mitogen-activated protein kinase extracellular signal-regulated kinase 1/2 pathway is involved in formyl-methionyl-leucyl-phenylalanine-induced p47phox phosphorylation in human neutrophils. J Immunol. 2000; 165:5238–5244. [PubMed: 11046057]

Dinauer MC, Deck MB, Unanue ER. Mice lacking reduced nicotinamide adenine dinucleotide phosphate oxidase activity show increased susceptibility to early infection with Listeria monocytogenes. J Immunol. 1997; 158:5581–5583. [PubMed: 9190903]

Fontayne A, Dang PM, Gougerot-Pocidalo MA, El-Benna J. Phosphorylation of p47phox sites by PKC alpha, beta II, delta, and zeta: effect on binding to p22phox and on NADPH oxidase activation. Biochemistry. 2002; 41:7743–7750. [PubMed: 12056906]

Goebel W, Kuhn M. Bacterial replication in the host cell cytosol. Curr Opin Microbiol. 2000; 3:49–53. [PubMed: 10679420]

Goldfine H, Johnston NC, Knob C. Nonspecific phospholipase C of Listeria monocytogenes: activity on phospholipids in Triton X-100-mixed micelles and in biological membranes. J Bacteriol. 1993; 175:4298–4306. [PubMed: 8331063]

Grundling A, Gonzalez MD, Higgins DE. Requirement of the Listeria monocytogenes broad-range phospholipase PC-PLC during infection of human epithelial cells. J Bacteriol. 2003; 185:6295–6307. [PubMed: 14563864]

Keith KE, Hynes DW, Sholdice JE, Valvano MA. Delayed association of the NADPH oxidase complex with macrophage vacuoles containing the opportunistic pathogen Burkholderia cenocepacia. Microbiology. 2009; 155:1004–1015. [PubMed: 19332803]

Lam GY, Huang J, Brumell JH. The many roles of NOX2 NADPH oxidase-derived ROS in immunity. Semin Immunopathol. 2010

Makino M, Kawai M, Kawamura I, Fujita M, Gejo F, Mitsuyama M. Involvement of reactive oxygen intermediate in the enhanced expression of virulence-associated genes of Listeria monocytogenes inside activated macrophages. Microbiol Immunol. 2005; 49:805–811. [PubMed: 16113511]

McCaffrey RL, Allen LA. Francisella tularensis LVS evades killing by human neutrophils via inhibition of the respiratory burst and phagosome escape. J Leukoc Biol. 2006; 80:1224–1230. [PubMed: 16908516]

McGilvray ID, Serghides L, Kapus A, Rotstein OD, Kain KC. Nonopsonic monocyte/macrophage phagocytosis of Plasmodium falciparum-parasitized erythrocytes: a role for CD36 in malarial clearance. Blood. 2000; 96:3231–3240. [PubMed: 11050008]

Mott J, Rikihisa Y, Tsunawaki S. Effects of Anaplasma phagocytophila on NADPH oxidase components in human neutrophils and HL-60 cells. Infection and immunity. 2002; 70:1359–1366. [PubMed: 11854221]

Myers JT, Tsang AW, Swanson JA. Localized reactive oxygen and nitrogen intermediates inhibit escape of Listeria monocytogenes from vacuoles in activated macrophages. J Immunol. 2003; 171:5447–5453. [PubMed: 14607950]

Prada-Delgado A, Carrasco-Marin E, Bokoch GM, Alvarez-Dominguez C. Interferon-gamma listericidal action is mediated by novel Rab5a functions at the phagosomal environment. The Journal of biological chemistry. 2001; 276:19059–19065. [PubMed: 11262414]

Remer KA, Reimer T, Brcic M, Jungi TW. Evidence for involvement of peptidoglycan in the triggering of an oxidative burst by Listeria monocytogenes in phagocytes. Clinical and experimental immunology. 2005; 140:73–80. [PubMed: 15762877]

Schnupf P, Portnoy DA. Listeriolysin O: a phagosome-specific lysin. Microbes Infect. 2007; 9:1176–1187. [PubMed: 17720603]

Shaughnessy LM, Hoppe AD, Christensen KA, Swanson JA. Membrane perforations inhibit lysosome fusion by altering pH and calcium in Listeria monocytogenes vacuoles. Cell Microbiol. 2006; 8:781–792. [PubMed: 16611227]

Shiloh MU, MacMicking JD, Nicholson S, Brause JE, Potter S, Marino M, Fang F, Dinauer M, Nathan C. Phenotype of mice and macrophages deficient in both phagocyte oxidase and inducible nitric oxide synthase. Immunity. 1999; 10:29–38. [PubMed: 10023768]

Sibelius U, Schulz EC, Rose F, Hattar K, Jacobs T, Weiss S, Chakraborty T, Seeger W, Grimminger F. Role of Listeria monocytogenes exotoxins listeriolysin and phosphatidylinositol-specific phospholipase C in activation of human neutrophils. Infect Immun. 1999; 67:1125–1130. [PubMed: 10024552]

Siemsen DW, Kirpotina LN, Jutila MA, Quinn MT. Inhibition of the human neutrophil NADPH oxidase by Coxiella burnetii. Microbes Infect. 2009; 11:671–679. [PubMed: 19379824]

Styrt B, Walker RD, White JC. Neutrophil oxidative metabolism after exposure to bacterial phospholipase C. J Lab Clin Med. 1989; 114:51–57. [PubMed: 2544653]

Titball RW. Bacterial phospholipases C. Microbiol Rev. 1993; 57:347–366. [PubMed: 8336671]

Vazquez-Torres A, Xu Y, Jones-Carson J, Holden DW, Lucia SM, Dinauer MC, Mastroeni P, Fang FC. Salmonella pathogenicity island 2-dependent evasion of the phagocyte NADPH oxidase. Science. 2000; 287:1655–1658. [PubMed: 10698741]

Highlights

- *L. monocytogenes* PLCs activate and LLO inhibits ROS production by NOX2 NADPH oxidase
- LLO-deficient bacteria survive in NOX2 NADPH oxidase-deficient macrophages and mice
- LLO inhibits NOX2 NADPH oxidase assembly at the phagosome
- LLO-related pore-forming cytolysin, PFO, can complement LLO-deficiency

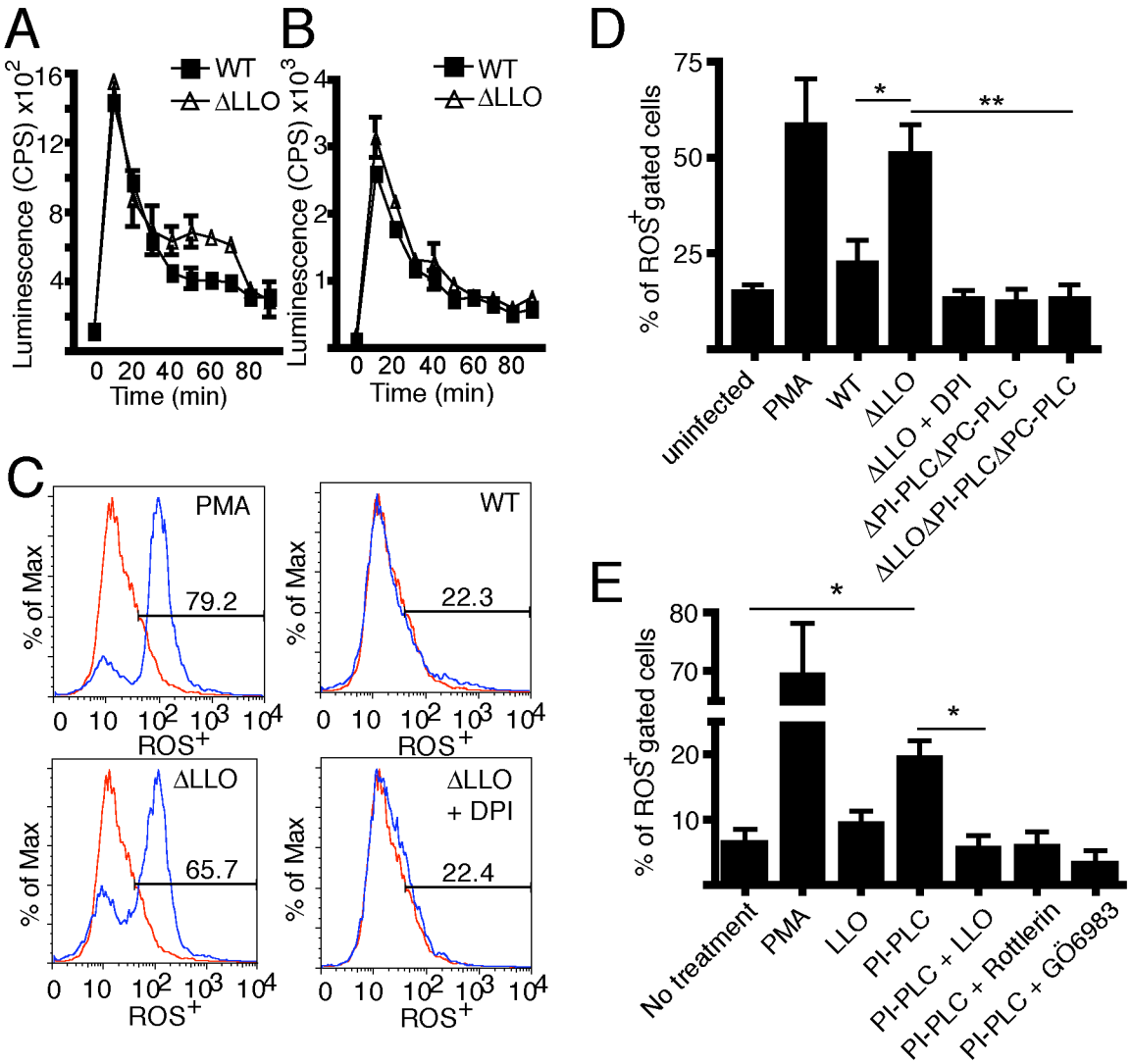

Figure 1. LLO inhibits PLC-mediated ROS production by the NOX2 NADPH oxidase

ROS production was assessed via (A) luminol or (B) isoluminol assay. BMDM were infected at an MOI of 10 with wild type (WT) or ΔLLO bacteria. The figures show data from one representative experiment done in duplicate where each data point represents the average and range. The experiment was performed a total of three independent times and the average and SEM is tabulated in Tables S1A and S1B. (C) RAW 264.7 macrophages were treated with PMA or infected with the indicated bacterial strain (MOI of 10) with or without DPI. Intracellular ROS production was assessed via flow cytometry with CM-H_2DCFDA, which was added 30 min p.i. and cells were analyzed at 60 min p.i.. Flow cytometry analysis was conducted on live cell populations, gated against a stained untreated control (red). Representative plots are shown. (D) Quantification of the percentage of ROS^+ cells in (C) for the indicated bacterial strains. Graph represents mean ± SEM from five independent experiments. (E) RAW 264.7 macrophages were treated with the indicated agents for 60 min and CM-H_2DCFDA dye was used to measure ROS production. Quantification of the percentage of ROS^+ cells was done using flow cytometry. Bars represent mean ± SEM from three independent experiments.

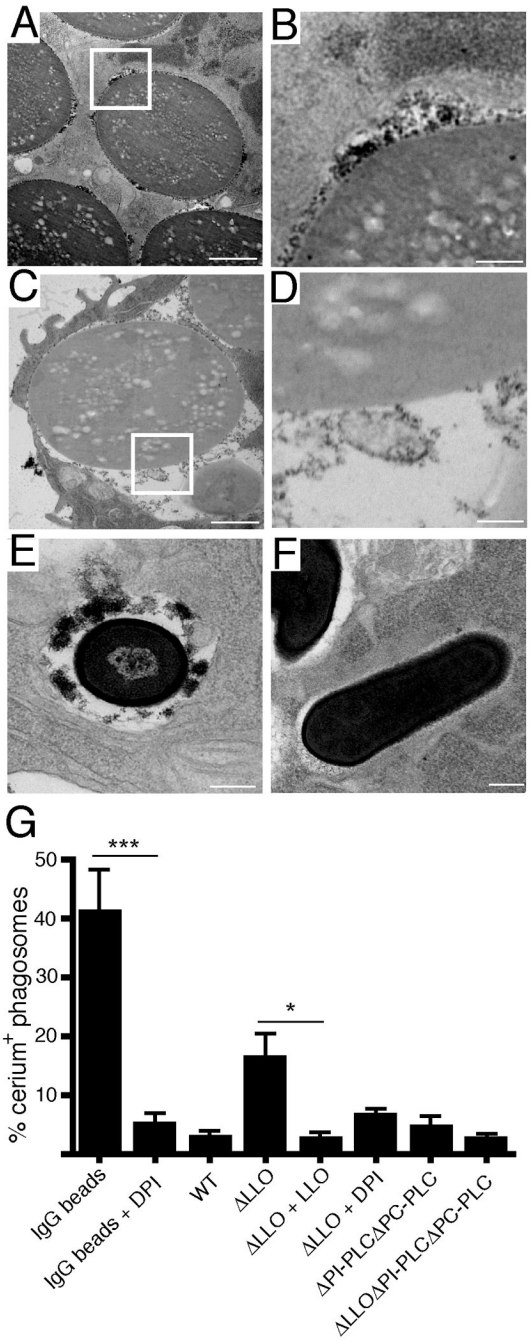

Figure 2. LLO inhibits ROS production in phagosomes

(A, B) Phagosomal production of ROS was assessed via transmission electron microscopy (TEM). RAW 264.7 macrophages were treated with IgG-coated latex beads in the presence of cerium chloride. Reduction of cerium chloride results in the formation of cerium perhydroxide precipitate. The presence of these electron-dense products in TEM was indicative of NOX2 NADPH oxidase production of ROS. (B) is a higher magnification view of the boxed region in (A). (C, D) Experiment conducted as in (A) and (B) but in the presence of DPI. (D) is a higher magnification view of the boxed region in (C). RAW 264.7 macrophages were infected with either WT or ΔLLO bacteria at MOI 10. (E) Representative TEM of a ΔLLO-containing phagosome at 60 min p.i.. (F) Representative TEM of a wild

type-containing phagosome at 60 min p.i.. (G) The percentage of cerium perhydroxide^{+} phagosomes at 60 min p.i. were quantified. One hundred phagosomes were assessed per sample from four independent experiments. Bars represent mean ± SEM. All scale bars are 1 μm.

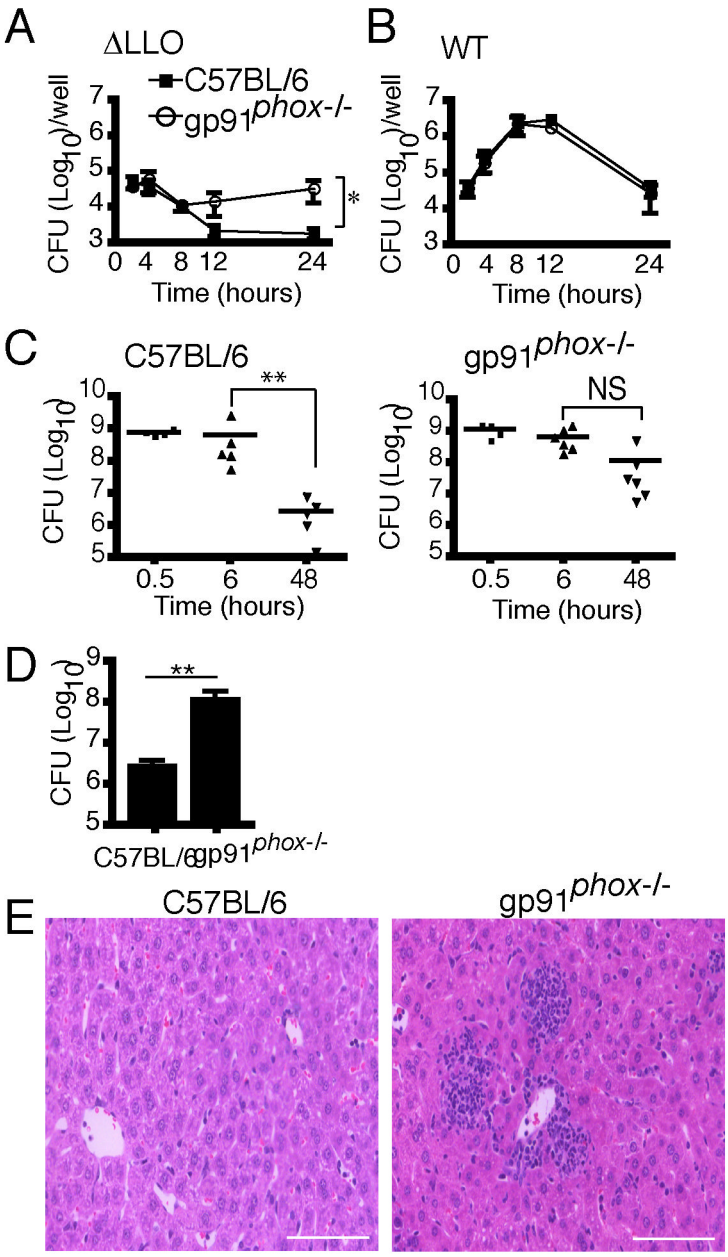

Figure 3. ΔLLO bacteria survive in NOX2 NADPH oxidase-deficient macrophages *in vitro* and *in vivo*

BMDM from C57BL/6 or gp91$^{phox-/-}$ mice were infected with ΔLLO (A) or WT (B) bacteria. The number of intracellular bacteria (colony forming units) was quantified via gentamicin protection assay at the indicated times. Data represent the mean ± SEM for three independent experiments. (C) C57BL/6 and gp91$^{phox-/-}$ mice were intravenously infected with 10^9 ΔLLO bacteria in a volume of 200μl. Mice were sacrificed at the indicated times and livers removed for quantification of bacterial load. Data represent results from three independent experiments with a total of six mice per condition per time point. Statistical analyses were performed using a non-parametric Mann-Whitney test to assess significance. NS = not significant. (D) Bacterial CFU in the liver (mean ± SEM) recovered at 48 h post-infection from C57BL/6 and gp91$^{phox-/-}$ mice from three independent experiments were

compared using the non-parametric Mann-Whitney test. (E) Liver sections from C57BL/6 and gp91$^{phox-/-}$ mice 24 h post-infection were embedded and mounted. Tissues were stained with hematoxylin and eosin (H&E) and representative images are shown. Scale bar, 100 μm.

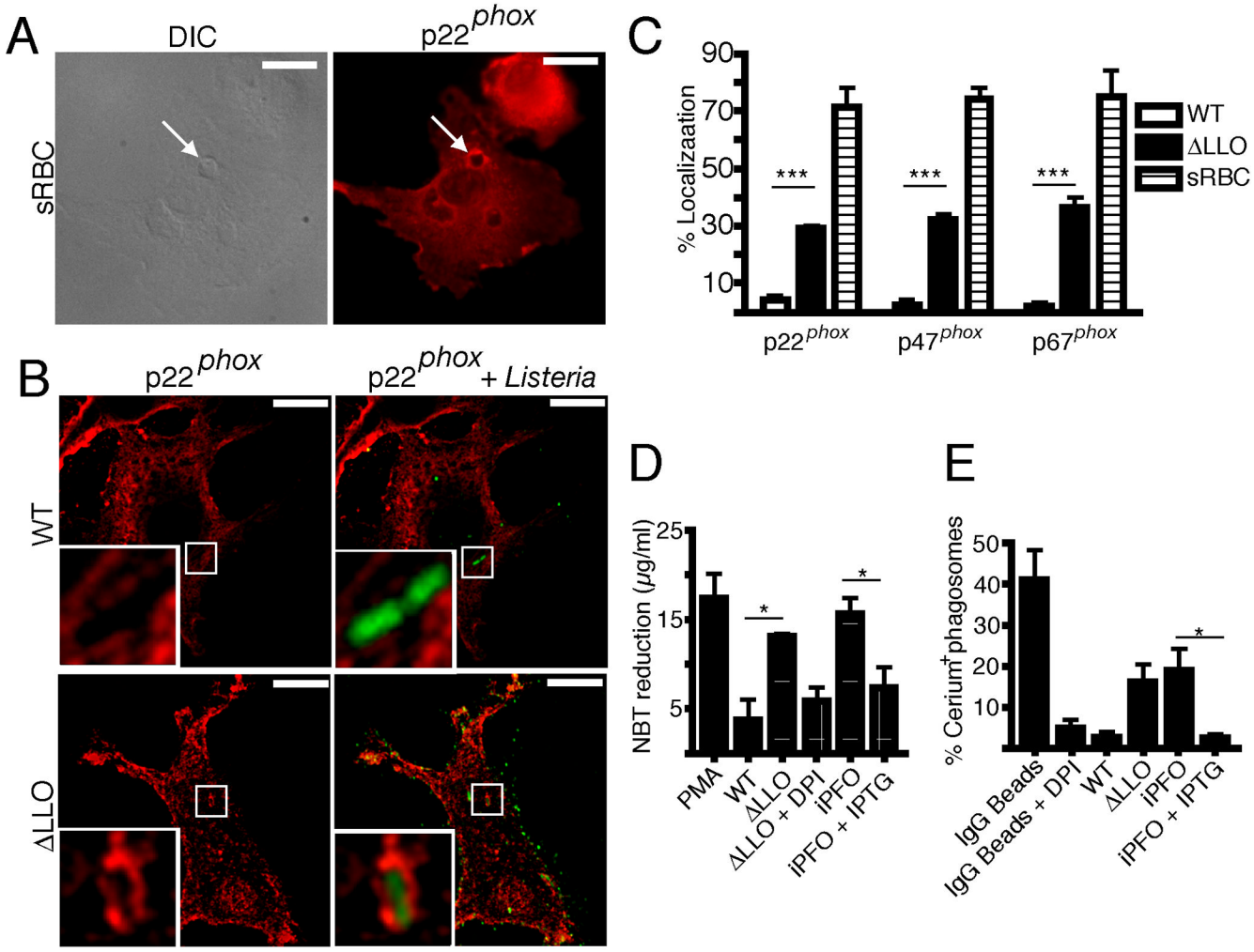

Figure 4. LLO inhibits NOX2 NADPH oxidase assembly at the phagosome and inhibition of ROS production can be complemented by perfringolysin O (PFO)

(A) Human macrophages were treated with IgG-opsonized sheep red blood cells (sRBC) for 60 min and fixed. Cells were then stained with anti-p22^{phox} antibodies. Differential interference contrast (DIC) microscopy and epifluorescence images were acquired. Arrows indicate colocalization of p22^{phox} with phagosomes. (B) Human macrophages were infected at MOI 10 with either wild type or ΔLLO bacteria for 60 min and fixed. Cells were then stained with anti-p22^{phox} antibodies in red and for bacterial-expressed GFP in green. Representative confocal z slices are shown. Insets are higher magnifications of the boxed areas. (C) Quantification of p22^{phox}, p47^{phox} or p67^{phox} colocalization with sRBC or bacteria containing phagosomes. One hundred phagosomes were assessed from each of the three independent experiments. Bars represent mean ± SEM. (D) Superoxide production by RAW 264.7 macrophages was measured by NBT reduction assay. Cells were either treated with PMA or infected at MOI 10 with wild type or ΔLLO bacteria for 30 min, followed by NBT treatment. Cells were also infected with iPFO, a complemented strain of ΔLLO that expresses PFO under an IPTG inducible promoter. Graph represents mean ± SEM from three independent experiments. (E) Cells were either treated with PMA or infected at MOI 10 with wild type or ΔLLO bacteria for 30 min, followed by cerium chloride treatment. TEM analysis was employed to quantify the percentage of phagosomes that were cerium

perhydroxide precipitate positive. One hundred phagosomes were assessed from each of the four independent experiments. Bars represent mean ± SEM. All scale bars are 10 μm.